Atmos. Chem. Phys. Discuss., 13, 2795–2833, 2013
www.atmos-chem-phys-discuss.net/13/2795/2013/
doi:10.5194/acpd-13-2795-2013

Atmospheric Chemistry and Physics Discussions

Brown carbon: a significant atmospheric absorber of solar radiation?

Y. Feng[1], **V. Ramanathan**[2], **and V. R. Kotamarthi**[1]

[1]Environmental Science Division, Argonne National Laboratory, Argonne, IL, 60439, USA
[2]Center for Cloud, Chemistry and Climate, Scripps Institute of Oceanography, University of California, San Diego, La Jolla, CA, USA

Received: 10 January 2013 – Accepted: 12 January 2013 – Published: 25 January 2013

Correspondence to: Y. Feng (yfeng@anl.gov)

Published by Copernicus Publications on behalf of the European Geosciences Union.

Abstract

Several recent observational studies have shown organic carbon aerosols to be a significant source of absorption of solar radiation. The absorbing part of organic aerosols is referred to as brown carbon. Comparisons with observations indicate that model-simulated aerosol absorption is under-estimated in global models, one of the reasons being the neglect of brown carbon. Using a global chemical transport model coupled with a radiative transfer model, we estimate for the first time the enhanced absorption of solar radiation due to "brown" carbon (BrC) in a global model. When BrC is included, the simulated wavelength dependence of aerosol absorption, as measured by the Angstrom exponent increases from 0.9 to 1.2 and thus agrees better with AERONET spectral observations at 440–870 nm. The resulting absorbing aerosol optical depth increases by 3–18 % at 550 nm and up to 56 % at 350 nm. The global simulations suggest that BrC contributes up to +0.25 $W m^{-2}$ or 19 % of the absorption by anthropogenic aerosols, of which 72 % is attributed to black carbon, and 9 % is due to sulfate and non-absorbing organic aerosols coated on black carbon. Like black carbon, the overall forcing of BrC at the top of the atmosphere (TOA) is a warming effect (+0.11 $W m^{-2}$), while the effect at the surface is a reduction or dimming (−0.14 $W m^{-2}$). Because of the inclusion of BrC in our model, the direct radiative effect of organic carbonaceous aerosols changes from cooling (−0.08 $W m^{-2}$) to warming (+0.025 $W m^{-2}$) at the TOA, on a global mean basis. Over source regions and above clouds, the absorption of BrC is more significant and thus can play an important role in photochemistry and the hydrologic cycle.

1 Introduction

Absorption of solar radiation by aerosols has a significant impact on the atmospheric energy distribution and hydrologic processes. By intercepting the incoming solar radiation before it reaches the surface, aerosols heat the atmosphere and in turn cool the

ACPD
13, 2795–2833, 2013

surface. Locally, this leads to reduction in cloud cover through evaporation and suppression of the upward motion for cloud formation; on larger scales, surface dimming due to strong aerosol absorption could decrease global mean evaporation and rainfall by weakening the radiative-convective coupling between the atmosphere and the surface (Ramanathan and Carmichael, 2008). The magnitude of the atmospheric forcing induced by anthropogenic absorbing aerosols, mainly black carbon (BC) emitted from combustion processes, has been suggested (Forster et al., 2007; Ramanathan and Carmichael, 2008) to be comparable to the atmospheric forcing by all greenhouse gases (GHGs). In addition to BC, mineral dust particles also absorb in the solar radiation spectrum. Although absorbing aerosols amplify the atmospheric forcing due to GHGs, their dimming effect compensates for the GHG warming at the surface. The short lifetimes of aerosols result in large variabilities in global and regional forcing. The significance and complexity of the climate impacts of absorbing aerosols highlight the importance of quantifying their radiative effects.

Model-simulated BC concentrations and aerosol absorption optical depth (AAOD) have been compared with surface and aircraft measurements such as the IMPROVE network (http://vista.cira.colostate.edu/improve), AERONET (Holben et al., 1998), and OMI satellite data (Torres et al., 2007). The model-data comparisons suggest that simulated BC surface concentrations, column loadings, and aerosol absorption are often under-estimated over regions. Model under-estimation can reach factors of 2 to 5, particularly over regions dominated by biomass burning, South and East Asia, and remote regions (Koch et al., 2009; Menon et al., 2010; Ganguly et al., 2012). Such large gaps between simulated and observed BC and aerosol absorption lead to disconcerting discrepancies in the estimated aerosol radiative forcing. Two earlier observationally constrained approaches inferred a global BC forcing of about 0.9 to 1.0 $W m^{-2}$ (Sato et al., 2003; Ramanathan and Carmichael, 2008). A more recent observational study by Chung et al. (2012) estimated a BC forcing of 0.65 (0.5 to 0.8) $W m^{-2}$, about 85 % larger than the Intergovernmental Panel on Climate Change (IPCC) model (Forster et al., 2007) estimate of 0.35 (0.2 to 0.6) $W m^{-2}$, and 30 % larger than post-IPCC model

ACPD
13, 2795–2833, 2013

study results (Jacobson, 2010; Andrews et al., 2010; Ming et al., 2010; Shindell et al., 2012), which are closer to 0.5 (±0.05) $W m^{-2}$. The direct absorption of sunlight by organic aerosols is typically ignored, except in a few studies (e.g. Jacobson, 2001).

Recently, optical and thermal analysis (e.g. Kirchstetter et al., 2004; Chen and Bond, 2010) and electron microscopy (e.g. Alexander et al., 2008) from laboratory and field experiments have provided strong evidence for the existence of a class of absorbing organic carbon (OC). This substance, known as brown carbon (BrC) for its light brownish color, absorbs strongly in the ultraviolet wavelengths and less significantly going into the visible (Kirchstetter et al., 2004; Hoffer et al., 2006). Types of BrC include tar materials from smoldering fires or solid fuel combustion (Bond, 2001; Alexander et al., 2008), pyrolysis products from biomass burning (Mukai and Ambe, 1986), or humic-like substances from soil or biogenic emissions (Limbeck et al., 2003). Depending on its origins, the absorption efficiency and spectral dependence of BrC varies (Andreae and Gelencsér, 2006). A few recent observationally based studies indicated an abundance of BrC in the atmosphere, which could enhance solar radiation absorption and reduce surface radiative flux substantially (Chung et al., 2012; Bahadur et al., 2012). From the AERONET refractive index retrievals, Arola et al. (2011) inferred significant amounts of BrC (10–35 $mg m^{-2}$) in Africa, South America, and South and East Asia. Park et al. (2010) used a 1 : 1 mass ratio for BC to approximate BrC concentrations over East Asia and derived values for regional-mean radiative forcing of BrC of about $-0.43 W m^{-2}$ at the surface and $0.05 W m^{-2}$ at the top of the atmosphere (TOA).

However, in many global climate models, organic compounds are still considered mainly as scattering aerosols. Their optical properties are approximated by either non-absorbing ammonium sulfate or weakly absorbing water-soluble aerosols (d'Almeida et al., 1991). Using a global chemical transport model and a Monte Carlo radiative transport model, we examine the enhancement in atmospheric absorption due to BrC for year 2000 emissions and present the first global estimate of its direct radiative forcing. The following section describes the global chemical transport model and a treatment for BrC optical properties. Section 3 compares the global calculations of aerosol

ACPD
13, 2795–2833, 2013

optical properties with available surface and satellite observations and discusses the contribution of BrC to aerosol direct radiative forcing. Finally, the main results of this study and implications for future work are summarized in Sect. 4.

2 Model description

2.1 Global chemical transport model

Global distributions of aerosol concentrations were simulated with a chemical transport model – a University of Michigan version of the Lawrence Livermore National Laboratory IMPACT model (Liu and Penner, 2002; Rotman et al., 2004; Liu et al., 2005). The global model has a horizontal resolution of $2^{\circ} \times 2.5^{\circ}$, with 26 vertical layers from the surface to the top of the TOA. Tracers are transported at a 1-h time step. The transport schemes and aerosol modules were fully described by Rotman et al. (2004) and Liu et al. (2005), while nitrate and ammonium aerosols were included later (Feng and Penner, 2007). We adopted a version of the IMPACT model used in Feng and Ramanathan (2010), which is coupled with the European Centre for Medium-Range Weather Forecasts 40-yr re-analysis (ERA-40) meteorological data fields for year 2001 (Uppala et al., 2005). The treatment for aerosols is summarized below, while other model physics are given in the Appendix.

In the IMPACT model, sulfate aerosol is represented in three size bins of radius $< 0.05\,\mu m$, 0.05–0.63 µm, and 0.63–1.26 µm. The concentrations of SO_2, SO_4^{2-}, H_2O_2, and dimethyl sulfide (DMS) were simulated with an online sulfur model (Liu and Penner, 2002; Liu et al., 2005). As indicated by Liu et al. (2007), gas-phase-produced sulfate mass was distributed to the three size bins on the basis of a continental sulfate aerosol size distribution (Chuang et al., 1997), and the sulfate produced in cloud was added to the second size bin as accumulation-mode aerosol. The size-segregated mass fluxes for sea salt and dust were calculated as dependent on wind speed, according to Monahan et al. (1986) and Ginoux et al. (2001), respectively. Once emitted, sea salt and

ACPD
13, 2795–2833, 2013

mineral dust aerosols were transported in four size bins (0.05–0.63 µm, 0.63–1.26 µm, 1.26–2.5 µm, and 2.5–10 µm). Carbonaceous aerosols, BC, and OC were considered in one size bin only (radius < 0.63 µm).

The content of BrC in OC generated from biofuel combustion and biomass burning sources is approximated by a fraction of 92 % for methanol-soluble absorbing OC, on the basis of a solid-fuel pyrolysis study (Chen and Bond, 2010). Organic solvents can dissolve most of the absorbing organics, including water-soluble OCs (Chen and Bond, 2010). In the IMPACT model, OC is converted to particulate organic matter at a ratio of 1 : 1.4 to account for secondary aerosol formation from volatile organic compounds. Therefore, the fractional BrC in total organic matter from biofuel and biomass emissions is about 66 % (= 92 % ÷ 1.4), while the other 34 % of the simulated organic matter mass is assumed to be non-absorbing or scattering only. Here, no BrC is considered in the fossil fuel-produced organic matter, as the high-temperature environment generally associated with fossil fuel combustion does not seem favorable for formation of BrC (Andreae and Gelencsér, 2006). This assumption is consistent with the results of observationally based studies, in which BrC is inferred to be most abundant over regions dominated by biofuel combustion or biomass burning (Arola et al., 2011). Naturally emitted OC might also be a source of primary BrC particles (Andreae and Gelencsér, 2006). This is not considered because of the level of uncertainty in the emissions.

Table 1 summarizes annual emissions and burdens of major aerosols and their lifetimes, calculated for year 2000. Anthropogenic SO_2 emissions are based on the EDGARv32 emission inventory (Olivier et al., 2001; Olivier and Berdowski, 2001). The gridded SO_2 is scaled by the ratio of the AeroCom global emission (Dentener et al., 2006) over that of EDGAR, for a total of 56.24 Tg S. Additional emissions of SO_2 include non-eruptive volcanoes (Dentener et al., 2006) and an oceanic DMS source (Kettle and Andreae, 2000). The emissions of BC and organic matter are from Bond et al. (2007), including fossil fuel, bio-fuel, and open biomass burning sources. Both BC (7.96 Tg C) and organic matter emissions (69.5 Tg) in this study are comparable to the AeroCom emissions (7.72 Tg BC; 67.5 Tg organic matter). As Table 1 shows, the

ACPD
13, 2795–2833, 2013

model-calculated aerosol burdens are in the ranges of the AeroCom model predictions for year 2000 (Kinne et al., 2006). In addition, the global burden of BrC aerosols is estimated to be 0.65 mg m^{-2}, more than three times the BC content (0.19 mg m^{-2}) in the atmosphere. The geographic distributions of simulated BrC and the fraction BrC/OC are shown in Fig. 1. Over the major biomass burning and biofuel combustion regions, the annual mean BrC loadings generally exceed 2 mg m^{-2}, and the fraction of BrC in total OC is high, above 40–50 %. The highest BrC burden about 15–20 mg m^{-2}, is in southern Africa, where the BrC fraction is also the largest, at over 70–80 %. The content of BrC in total organic aerosols is low, at 20–40 %, in fossil-fuel-dominated eastern North America and Western Europe, as well as in major natural organic source regions in South America and South and East Asia.

2.2 Optical properties of brown carbon

Aerosol optical properties (specific extinction, single-scattering albedo (SSA), and asymmetry factor) are calculated from the Mie theory (Bohren and Huffman, 1983). Here two sets of the refractive index of BrC are derived to match the observed absorption cross sections – at 550 nm, 0.08 m^2 g^{-1} for the moderately absorbing BrC (Chen and Bond, 2010) and $\sim$ 0.7 m^2 g^{-1} for the strongly absorbing BrC (Kirchstetter et al., 2004). Table 2 lists the values in this study for absorption cross section (m^2 g^{-1}) and the derived refractive index at 350–650 nm. In the Mie calculations, the density of BrC is 1.569 g cm^{-3}, and the real part of its refractive index is 1.65 (Hoffer et al., 2006). A typical size distribution of fuel combustion aerosols is used with a mean diameter of 100 nm and standard deviation of 1.5 (Bond and Bergstrom, 2006). For the optical properties of BrC listed in Table 2, the absorption Angstrom exponent (AAE), defined as:

$$\mathrm{AAOD}(\lambda) \sim \lambda^{-\mathrm{AAE}} \quad (1)$$

ACPD
13, 2795–2833, 2013

is about 6.6 to 11. The wavelength λ is in nm. This calculated spectral dependence of aerosol absorption is consistent with that observed for BrC (Kirchstetter and Thatcher, 2012).

The refractive indices for other aerosol species are the same as in Feng and Ramanathan (2010). To account for enhanced absorption of carbonaceous particles due to coating acquired in the aging process, a core-shell configuration (Bohren and Huffman, 1983) is implemented in the calculation of optical properties for fossil fuel, biofuel, and biomass burning aerosols. The core is assumed to be strongly absorbing BC with a refractive index of $1.8 + i0.74$ (Bond and Bergstrom, 2006). The outer shell consists of non-absorbing sulfate and OC for fossil fuel aerosols, versus absorbing BrC and non-absorbing OC for biofuel and biomass burning aerosols, respectively. This core-shell configuration represents the likely aerosol mixtures on the basis of their origins, because of a lack of information on the aerosol mixing state given by the global model. Mie calculations were performed offline for a number of BC, OC, BrC, and sulfate mixtures and relative humidity (RH) values; a lookup table was generated and used in the global calculations. Climatological aerosol size distributions are used for fossil fuel and biofuel aerosols (Radke et al., 1988) and for biomass burning aerosols (Anderson et al., 1996), respectively. Dust and sea salt are assumed to be mixed externally.

Figure 2 shows the calculated absorption cross section ($m^2\,g^{-1}$ BC) at 550 nm for dry absorbing aerosols by source. The coating effect on BC particles enhances the aerosol absorption by a factor of 3 to 6 from that calculated for single BC spherules ($4\,m^2\,g^{-1}$), when the mass ratio of core (BC) versus shell is approximately 1 : 20 (equivalent to 1 : 2.7 in radius, if same density is assumed for core and shell materials). For the same thickness of shell, the largest enhancement is introduced by BrC coatings, compared to sulfate or non-absorbing OC. For hygroscopic sulfate, the coating effect could be amplified further by water uptake. For example, at RH = 80 %, an absorption cross section with a mass ratio of 4 : 1 for sulfate: BC is estimated at about $9.1\,m^2\,g^{-1}$ BC, versus $8.4\,m^2\,g^{-1}$ BC at RH = 0 %. Bond and Bergstrom (2006) and Bond et al. (2006) suggested that lower bounds of absorption are $5\,m^2\,g^{-1}$ for observed submicron BC

ACPD
13, 2795–2833, 2013

particles and 7.5 $m^2 g^{-1}$ for freshly emitted aggregates. They also indicated that simple aerosol models might improve aerosol optics by assuming that absorption increases linearly as non-absorbing aerosol condenses, reaching a maximum 1.5 times greater (i.e. 7.5 $m^2 g^{-1}$ times 1.5 = 11.25 $m^2 g^{-1}$) when particle volume has increased up to a factor of about six. Their recommended enhancement due to non-absorbing coatings (gray shaded areas in Fig. 2) is largely approximated by our parameterization for sulfate and non-absorbing OC coatings.

3 Global results

3.1 Aerosol optical depth and single-scattering albedo at 550 nm

The model-calculated annual mean aerosol optical depth (AOD) at 550 nm is compared in Fig. 3 with the MODIS/Terra satellite observations (MOD08 Level 3) for year 2001. The global model simulations capture the observed aerosol hot spots identified by the local maximum in the MODIS AOD, such as eastern China (> 0.5), northern India and the Arabian Sea (0.3–0.6), and north-central Africa (0.3–0.5). Agreement in AOD is also found in most of Europe and North America, where the prevailing annual mean AOD is low, at about 0.2. Both modeled and observed AOD values have similar spatial patterns over the ocean, ranging from 0.1 to 0.3, with higher values in the high-wind regions (due to sea salt) or downwind from continental pollution. Compared with the MODIS, the IMPACT model under-predicts in areas of south-central Africa, Amazon forests, and South and East Asia dominated by biomass burning and over-predicts in volcano-influenced regions of South America and Indonesia. These model biases might be related to uncertainty in aerosol emissions, because most of the discrepancies occur near those source regions. The calculated global and annual mean AOD is 0.132, within 3 % of the MODIS retrieval (0.128). Such agreement between the model AOD and satellite observations helps to constrain the estimation of aerosol radiative forcing in the next section.

ACPD
13, 2795–2833, 2013

Figure 4 compares the monthly mean SSA at 550 nm from the model calculations and the AERONET data. The AERONET SSA values shown are calculated from the AERONET V2 Inversion products Level-2 daily data at 440 nm and 675 nm (Dubovik et al., 2006). For computation of the monthly means, we selected only the AERONET sites with at least 10 daily measurements for each month during the 20 yr from 1992 to 2012. The SSA monthly predictions correlate with the AERONET observations (a total of 1061 data points) with a coefficient of 0.51. The mean percentage error and bias between the modeled (without BrC) and observed SSA values are small, at about −2 % and 3 %, respectively. Regionally, the model results indicate that aerosols are generally more absorbing in biomass burning regions (SSA = 0.87–0.91) and South and East Asia (0.92–0.94) than over Europe and North America (∼ 0.95), which is similarly revealed in the AERONET data. In dust-influenced central Africa, however, the predicted mean SSA is about 0.95, larger than the mean retrieval of 0.92 from AERONET.

3.2 Effects of brown carbon on aerosol spectral absorption

The consideration of BrC increases total aerosol absorption. In Fig. 4, the two model simulations with BrC (denoted by solid circles and open squares) predict lower SSA values at 550 nm than the simulation without BrC (cross symbols), especially in areas of South America and southern Africa dominated by biomass burning (colored in green). Although the changes in SSA are small at about 1–2 %, the resulting enhancement in AAOD is more significant, as illustrated in Fig. 5. The annual mean AAOD (×100) at 550 nm is increased by 0.2 to 2, especially over biomass burning or biofuel combustion regions, where the AAOD simulated by large-scale models is often underestimated compared to observations (Koch et al., 2009). In the Southern Hemisphere, the percent increase in AAOD due to BrC is about 20–40 % of the total AAOD, more substantial than the contribution of BrC in the Northern Hemisphere, where absorbing aerosols of other types (BC and dust) are also abundant. On the other hand, originating mainly from biofuel consumption rather than open vegetation burning as in the

ACPD
13, 2795–2833, 2013

Southern Hemisphere, BrC in the Northern Hemisphere would have a large impact in densely populated areas, and its impact is likely to continue increasing in the future in the absence of emission controls for biofuels. At 550 nm, the inclusion of BrC enhances the global and annual mean AAOD by +3 % to +18 % (Table 3), depending on the absorption efficiency of BrC.

At the shorter wavelengths, BrC is a stronger and thus more important absorber than at 550 nm. Without BrC, the calculated AAE at 440–870 nm is mostly below 1.125, with a mean of 0.9 over the AERONET sites (excluding those near deserts). This calculated absorption spectral dependence without BrC represents BC particles coated with non-absorbing sulfate or organic substances as simulated by the model. This value is generally weaker than the AAE inferred from the AERONET data, which extends from 0.625 to 2 and has a mean value of 1.2. When BrC absorption is taken into account, the calculated AAOD is enhanced by 8–26 % at 450 nm and by up to 56 % at 350 nm (Table 3). As a result, the augmented absorption at smaller wavelengths leads to much larger AAE values for carbonaceous aerosols.

In Fig. 6, the frequency distribution of the simulated AAE is shown with AERONET retrievals for different regions. Except over biomass-dominated South America and southern Africa, the model simulations (including the strongly absorbing BrC) agree best with the observations, while the simulated AAE values without BrC are generally low-biased. Although no BrC is explicitly assumed to be associated with fossil fuel combustion, the AAE distribution is in good agreement over Europe and North America, which are dominated by fossil fuel emissions. However, the simulated AAE over East Asia and South Asia is on the low end of the AERONET retrievals, even with the strongly absorbing BrC. This might be because the BrC in Asia has stronger absorption efficiency than the values reported by Kirchstetter et al. (2004) and Chen and Bond (2010). For instance, the tar balls (one of the common physical form of BrC) collected in the East Asian-Pacific outflow are suggested to be highly absorptive (Alexander et al., 2008); this substance has a mean refractive index with an imaginary part of 0.27 at 550 nm, 10 times the value for the strongly absorbing BrC used in this study. Over

ACPD
13, 2795–2833, 2013

the biomass burning regions, the AAE is over-predicted, although the absorption cross section used for BrC is similar to that from biomass burning aerosol samples (Kirchstetter et al., 2004). This could be because the assumed fraction of BrC in total OC (92 %) is too high for open biomass burning aerosols.

Our calculations of the BrC spectral absorption are consistent with several recent observationally based studies. Kirchstetter and Thatcher (2012) showed that BrC (or absorbing OC) contributes 49 % of the ultraviolet absorption by particulate matter below 400 nm, on the basis of a spectroscopic analysis of 115 wood smoke samples. In comparison, the contribution of strongly absorbing BrC to global AAOD at 350 nm is estimated at about 36 % (Table 3). An analysis of AERONET data by Russell et al. (2010) suggested that the observed AAE values at 440–870 nm are between 0.8 and 1.4 for urban sites (similar to Fig. 6a), and about 1.2–1.6 for biomass burning regions (similar to Fig. 6b). By applying an analytical partitioning method to the AERONET AOD and SSA values at 440 nm, 675 nm, and 870 nm, Bahadur et al. (2012) found that the BrC on average contributes 28 % to the total aerosol absorption at 440 nm, while our estimate is about 20 % (Table 3).

Figure 7 demonstrate that the calculated AAE (for strongly absorbing BrC) between 440 nm and 675 nm varies as a function of OC : BC burden. When OC is absent (OC/BC = 0), the AAE for pure BC is approximatedly 0.53, identical to the value of 0.55 ± 0.24 estimated by Bahadur et al. (2012). In the global simulations, there is no pure BC, so the minimum AAE is about 0.825. Most of the model columns have OC/BC ratios ranging between 1 and 12. As the fraction of OC increases, the calculated AAE increases to values around 1.5 to 2. Because the absorption by BrC is close to zero near 675 nm, the best-fit curve (solid red line) in Fig. 7 could be used to estimate the enhancement of AAOD due to BrC at the smaller wavelengths in models that only consider BC, as a function of the estimated OC/BC fractions and aerosol absorption at 675 nm.

ACPD
13, 2795–2833, 2013

3.3 Aerosol direct radiative forcing

Direct radiative forcing by aerosols is estimated with the Monte Carlo Aerosol, Cloud and Radiation (MACR) model (Podgorny and Ramanathan, 2001; Kim and Ramanathan, 2008) for the predicted monthly mean aerosol optical properties. The MACR radiation model uses 25 bands to cover the solar spectrum from 0.25 mm to 5.0 mm with 50 layers (Vogelmann et al., 2001). The International Satellite Cloud Climatology Project satellite cloud cover and optical depth for low, middle, and high clouds were used in calculations of all-sky radiative flux (Kim and Ramanathan, 2008). These values were interpolated to the T42 grid (approximately 2.8° by 2.8°) as input fields to the MACR model, as well as the compiled monthly ozone, water vapor, and surface albedo data for the simulated year (Kim and Ramanathan, 2008).

Aerosol radiative forcing is estimated as the difference in the calculated radiative fluxes with and without aerosols. Figure 8 shows the calculated annual mean all-sky direct radiative forcing by BrC and organic aerosols (OAs) without and with BrC for the year 2000 aerosol emissions. In Fig. 8a, the TOA forcing by BrC is positive globally, suggesting a general warming effect due to absorption of incoming solar radiation by BrC. On a global mean basis, BrC enhances total aerosol absorption by 7 % or 19 %, for moderately or strongly absorbing efficiencies, respectively (Table 4). The magnitude of the BrC absorption (about 0.1–0.25 $W m^{-2}$) is comparable to roughly one-quarter of the estimated atmospheric forcing of BC (1.07 $W m^{-2}$). The global forcing of BrC is about 0.04–0.11 $W m^{-2}$ at the TOA, while the effect at the surface is negative, ranging from $-0.06 W m^{-2}$ to $-0.14 W m^{-2}$. Regionally, these effects are more substantial. Figure 8a shows that the TOA forcing by BrC is above 0.25 $W m^{-2}$ over the major source regions, including the subtropical southern Africa and South America, South Asia and East Asia, which are dominated by biomass and bio fuel burning.

When BrC is not considered, OA consist of non-absorbing OC and other scattering substances. Thus, the TOA forcing by OA is negative over most of the domain, expect for regions overlapping with marine low-level clouds and in high latitudes, as shown

ACPD
13, 2795–2833, 2013

in Fig. 8b. Although OA does not absorb any solar radiation without BrC, they could still enhance the BC absorption by coating the BC particles. Especially over sea ice in high latitudes or above clouds (a bright surface with large surface albedo), small absorption ($\sim 0.5\,W\,m^{-2}$) due to the coating effect could cause a positive TOA forcing ($\sim 0.1\,W\,m^{-2}$). When the absorbing BrC is included as OA, it reduces the strong negative TOA forcing of OA, while increasing the weak positive forcing (Fig. 8c). The global mean OA direct radiative forcing is thus changed by BrC from an overall negative effect ($-0.086\,W\,m^{-2}$) to a positive forcing ($+0.025\,W\,m^{-2}$).

The changes in the OA direct radiative forcing caused by BrC have significant implications on regional scales. Over central eastern China and Europe, the radiative impact of total OA with BrC might amplify (rather than offsetting, as originally estimated) the warming due to BC emitted from the same anthropogenic sources by adding an additional $0.25\,W\,m^{-2}$ of warming. This implies that emission controls on fuel combustion should also include organic carbonaceous aerosols in addition to BC. Futher, BrC in biomass burning aerosols from the African savannas strongly intensifies the positive forcing of OA off the western coast of central Africa, which is often overlaid with subtropical stratocumulus cloud decks. The nearly-zero direct radiative forcing of OA at 30° S–5° N and 20° W–5° E is changed by BrC to a moderately positive forcing of $0.29\,W\,m^{-2}$, which could significantly alter regional cloud and precipitation formation related to the African monsoon (e.g. Huang et al., 2009; Sakaeda et al., 2011). Over mid-latitude oceans and higher altitudes, the weakly positive TOA forcing by OA is nearly doubled by transported BrC. Although the absolute aerosol forcing is small ($0.1–0.25\,W\,m^{-2}$) in the polar regions, the high-altitude climate is highly sensitive to aerosol perturbations (Shindell and Faluvegi, 2009).

Figure 9 shows that under clear sky, the BrC direct radiative forcing without cloud masks is larger over the land, where aerosols are mostly below clouds; on the other hand, the radiative impact of BrC transported over the ocean is less in the clear sky, because there is no amplified absorption from the reflection of clouds underneath. As a result, the clear-sky TOA forcing of OA is predominately more negative than under

ACPD
13, 2795–2833, 2013

cloudy sky, either with or without BrC. The global effect of BrC on the clear-sky OA forcing ($+0.09\,W\,m^{-2}$) is slightly less than in all sky conditions ($+0.11\,W\,m^{-2}$).

The TOA forcing by all anthropogenic aerosols is estimated at about $-0.17\,W\,m^{-2}$ in the present study (Table 4). This value is similar to the AeroCom model estimate of $-0.21 \pm 0.20\,W\,m^{-2}$ with similar emissions[1] (Schulz et al., 2006). The estimated total atmospheric absorption ($+1.47\,W\,m^{-2}$) and surface dimming ($-1.64\,W\,m^{-2}$) by aerosols are more significant – roughly 80 % and 38 % larger than the AeroCom means, respectively. Other anthropogenic aerosols, including sulfate and non-absorbing organic matter, could also increase aerosol absorption by coating BC particles. The estimated enhancement due to the non-absorbing aerosol coating effect adds another 9 % to the total absorption. Compared with the observationally constrained estimate ($3.0\,W\,m^{-2}$) of Ramanathan and Carmichael (2008), the global calculations that include strongly absorbing BrC still under-estimate the atmospheric absorption ($1.47\,W\,m^{-2}$). One of the reasons might be under-predicted aerosol loadings; we note that the AOD comparison with MODIS satellite data in Fig. 3 indicates under-estimations in biomass burning regions.

Seasonal variations in the predicted burden and atmospheric forcing of BrC are shown in Fig. 10 for three locations with high BrC content. Similar to the BrC burdens inferred from the AERONET data (Arola et al., 2011), the model predictions peak in July-August-September at the two open biomass burning locations in South America (Alta Floresta, Brazil) and southern Africa (Mongu, Zambia), and the predicted burdens are also in similar ranges (about 5–15 $mg\,m^{-2}$). However, the estimated BrC is significantly low-biased in Kanpur, India, compared to the observationally based estimate. This is probably because BC emissions in South Asia might have been increasing during the past two decades (Bond et al., 2007); these emission increases might not be included in the global emission inventories for year 2000 used here. As for the atmospheric

[1]The AeroCom forcing quoted is the sum of the AeroCom anthropogenic aerosol forcing, $-0.22 \pm 0.16\,W\,m^{-2}$, and biomass burning aerosol forcing, $0.01 \pm 0.04\,W\,m^{-2}$ (Schulz et al., 2006), because we consider open biomass burning aerosols as anthropogenic sources.

ACPD
13, 2795–2833, 2013

burden, the predicted BrC forcing depicts a strong seasonal cycle, peaking during the dry burning seasons in both hemispheres (Fig. 10). The maximum monthly forcing by BrC is about 5 $W m^{-2}$ at the southern African site in September.

4 Conclusions

Increasing evidence points to the existence of BrC in the atmosphere. The strong wavelength dependence from the ultraviolet to the visible in the observed carbonaceous aerosol absorption (AAE > 2) cannot be explained by mixing of BC with other scattering aerosols. Several observationally based studies have inferred the absorption cross section of BrC on the basis of multi-wavelength absorption measurements and have demonstrated significant absorption attributed to BrC in the ultraviolet and visible in laboratory studies or over observational sites (e.g. Kirchstetter et al., 2004; Chen and Bond, 2010; Bahadur et al., 2012; Kirchstetter and Thatcher, 2012). By integrating ground-based aerosol data with field and satellite observations, Chung et al. (2012) found that the global OA radiative forcing is close to zero when the contribution of BrC is implicitly included in the aerosol absorption spectrum. However, whether BrC could play a significant role in global and regional direct radiative forcing of carbonaceous aerosols remains uncertain.

We examined the enhancement in the absorption of solar radiation due to BrC with emissions compiled for year 2000 and generated the first estimate of global direct radiative forcing by BrC. Given the large variability in the observed absorption cross section (Chen and Bond, 2010), we derived two sets of refractive index data to represent the moderately and strongly absorbing BrC types.

The main findings of this study are as follows:

1. The inclusion of both BrC absorption properties leads to stronger wavelength dependence in the calculated aerosol absorption. The simulated aerosol AAE increases from 0.9 without BrC, to 1.0 with moderately absorbing BrC, and to 1.2

ACPD
13, 2795–2833, 2013

with strongly absorbing BrC; the last value agrees best with AERONET spectral retrievals.

2. The enhancement in the global mean AAOD due to BrC is up to 18 % at 550 nm, and it increases drastically to 56 % at 350 nm. This enhanced absorption of solar radiation by aerosols in the ultraviolet and near visible could imply a large impact on photolysis reaction rates and ozone photochemistry.

3. Model simulations suggest that the inclusion of BrC results in forcing of $+0.11\,W\,m^{-2}$ at the TOA. This changes the global radiative effect of organic carbonaceous aerosols from cooling ($-0.086\,W\,m^{-2}$) to warming ($+0.025\,W\,m^{-2}$), with much larger impact on regional climate. Therefore, failure to include the atmospheric heating ($+0.25\,W\,m^{-2}$) and surface dimming ($-0.14\,W\,m^{-2}$) by strongly absorbing BrC in climate simulations could introduce a significant source of uncertainty.

4. While BC is still the main absorber of solar radiation – contributing 72 % of the global atmospheric absorption – the contribution of BrC to aerosol forcing is > 20–50 % over regions dominated by seasonal biomass burnings and biofuel combustion, and more than a quarter of the estimated radiative effects of BC on a global basis.

5. The atmospheric burden of BrC is estimated to be $0.65\,mg\,m^{-2}$, which is more than three times the burden of BC. Since most of the BrC is associated with biomass burning aerosols, BrC aerosols are more likely to be elevated high above clouds and transported long distances than are the surface-emitted aerosols, leading to more widespread and efficient warming.

With respect to BrC, there are still large uncertainties regarding to its sources, formation, chemical composition, absorption properties, and scavenging process (thus lifetime). In the present study, we simplified BrC production by assigning 92 % of biomass and biofuel burning OC mass as BrC, on the basis of a study of solid fuels (Chen and

ACPD
13, 2795–2833, 2013

Bond, 2010). This fraction might be close to a possible maximum of BrC in total carbon. If that assumption holds, the contribution of BrC to atmospheric absorption would not exceed the predicted 19 % on a global and annual basis. In addition, the uncertainty in the measured absorption cross section for BrC (moderately or strongly absorbing) might cause differences of about 12 %. However, the absolute radiative impact of BrC could still be larger than the present estimates. For example, under-estimation could arise from under-predicted biomass burning or biofuel aerosol emissions, along with uncertainty in representing aerosol size and mixing state.

Therefore, the first global estimates of BrC radiative forcing in this study might demonstrate that BrC is an important atmospheric absorber, globally or regionally. These estimates should also motivate further efforts to quantify BrC in the atmosphere and to reduce the gap in aerosol absorption values between observationally based and global modeling studies.

Appendix A

The IMPACT model uses a flux-form semi-Lagrangian advection scheme (Lin and Rood, 1996). Aerosol dry and wet deposition are based on a resistance-in-series parameterization (Zhang et al., 2001) and the Harvard wet scavenging model (Liu et al., 2001), respectively. In convective updrafts, the fraction of tracer scavenged is calculated by the conversion rate of cloud condensate to precipitation ($0.005\,s^{-1}$) and the scavenging efficiency (fraction of tracer present in the cloud condensate). The scavenging efficiencies of sulfate, nitrate, ammonium, and carbonaceous aerosol are 1.0, 1.0, 1.0, and 0.4, respectively. The rainout rate depends on the tracer scavenging efficiency, the precipitating fraction of the grid box, and the conversion rate of cloud condensate to precipitation. Washout rate by large-scale precipitation is computed by a constant scavenging efficiency, $0.1\,mm^{-1}$, multiplied by the precipitation rate (in $mm\,h^{-1}$) (Balkanski et al., 1993). Resuspension is calculated in any grid box with net evaporation

ACPD
13, 2795–2833, 2013

of precipitation. Cumulus transport was derived from the relaxed Arakawa–Schubert scheme, as described in Penner et al. (1998).

Acknowledgements. Support for this research was provided to YF and VK by Argonne National Laboratory under US Department of Energy contract DE-AC02-06CH11357. VR's contribution to this study was supported by the National Science Foundation (Grant AGS1016496). All of the numerical simulations were performed by using the National Energy Research Scientific Computing Center's CrayXE6 Hopper.

References

Alexander, D. T. L., Crozier, P. A., and Anderson, J. R.: Brown carbon spheres in East Asian outflow and their optical properties, Science, 321, 833–836, doi:10.1126/science.1155296, 2008.

Anderson, B. E., Grant, W. B., Gregory, G. L., Browell, E. V., Collins Jr., J. E., Sachse, G. W., Bagwell, D. R., Hudgins, C. H., Blake, D. R., and Blake, N. J.: Aerosols from biomass burning over the tropical South Atlantic region: distributions and impacts, J. Geophys. Res., 101, 24117–24138, doi:10.1029/96JD00717, 1996.

Andreae, M. O. and Gelencsér, A.: Black carbon or brown carbon? The nature of light-absorbing carbonaceous aerosols, Atmos. Chem. Phys., 6, 3131–3148, doi:10.5194/acp-6-3131-2006, 2006.

Andrews, T., Forster, P. M., Boucher, O., Bellouin, N., and Jones, A.: Precipitation, radiative forcing and global temperature change, Geophys. Res. Lett., 37, L14701, doi:10.1029/2010GL043991, 2010.

Arola, A., Schuster, G., Myhre, G., Kazadzis, S., Dey, S., and Tripathi, S. N.: Inferring absorbing organic carbon content from AERONET data, Atmos. Chem. Phys., 11, 215–225, doi:10.5194/acp-11-215-2011, 2011.

Bahadur, R., Praveen, P. S., Xu, Y., and Ramanathan, V.: Solar absorption by elemental and brown carbon determined from spectral observations, P. Natl. Acad. Sci. USA, 109, 17366–17371, doi:10.1073/pnas.1205910109, 2012.

Balkanski, Y. J., Jacob, D. J., Gardner, G. M., Graustein, W. M., and Turekian, K. K.: Transport and residence times of continental aerosols inferred from a global 3-dimensional simulation of ^{210}Pb, J. Geophys. Res., 98, 20573–20586, 1993.

ACPD

13, 2795–2833, 2013

Bohren, C. F. and Huffman, D.: Absorption and Scattering of Light by Small Particles, Wiley, New York, 530 pp., 1983.
Bond, T. C.: Spectral dependence of visible light absorption by carbonaceous particles emitted from coal combustion, Geophys. Res. Lett., 28, 4075–4078, 2001.
Bond, T. C. and Bergstrom, R. W.: Light absorption by carbonaceous particles: an investigative review, Aerosol Sci. Tech., 40, 27–67, 2006.
Bond, T. C., Habib, G., and Bergstrom, R. W.: Limitations in the enhancement of visible light absorption due to mixing state, J. Geophys. Res., 111, D20211, doi:10.1029/2006JD007315, 2006.
Bond, T. C., Bhardwaj, E., Dong, R., Jogani, R., Jung, S., Roden, C., Streets, D. G., and Trautmann, N. M.: Historical emissions of black and organic carbon aerosol from energy-related combustion, 1850–2000, Global Biogeochem. Cy., 21, GB2018, doi:10.1029/2006GB002840, 2007.
Chen, Y. and Bond, T. C.: Light absorption by organic carbon from wood combustion, Atmos. Chem. Phys., 10, 1773–1787, doi:10.5194/acp-10-1773-2010, 2010.
Chuang, C. C., Penner, J. E., Taylor, K. E., Grossman, A. S., and Walton, J. J.: An assessment of the radiative effects of anthropogenic sulfate, J. Geophys. Res., 102, 3761–3778, 1997.
Chung, C. E., Ramanathan, V., and Decremer, D.: Observationally constrained estimates of carbonaceous aerosol radiative forcing, P. Natl. Acad. Sci. USA, 109, 11624–11629, 2012.
d'Almeida, G. A., Koepke, P., and Shettle, E. P.: Atmospheric Aerosols: Global Climatology and Radiative Characteristics, A. Deepak Pub., Hampton, VA, 1991.
Dentener, F., Kinne, S., Bond, T., Boucher, O., Cofala, J., Generoso, S., Ginoux, P., Gong, S., Hoelzemann, J. J., Ito, A., Marelli, L., Penner, J. E., Putaud, J.-P., Textor, C., Schulz, M., van der Werf, G. R., and Wilson, J.: Emissions of primary aerosol and precursor gases in the years 2000 and 1750 prescribed data-sets for AeroCom, Atmos. Chem. Phys., 6, 4321–4344, doi:10.5194/acp-6-4321-2006, 2006.
Dubovik, O., Sinyuk, A., Lapyonok, T., Holben, B. N., Mishchenko, M., Yang, P., Eck, T. F., Volten, H., Muñoz, O., Veihelmann, B., van der Zande, W. J., Leon, J.-F., Sorokin, M., and Slutsker, I.: Application of spheroid models to account for aerosol particle nonsphericity in remote sensing of desert dust, J. Geophys. Res., 111, D11208, doi:10.1029/2005JD006619, 2006.

ACPD
13, 2795–2833, 2013

Feng, Y. and Penner, J. E.: Global modeling of nitrate and ammonium: Interaction of aerosols and tropospheric chemistry, J. Geophys. Res., 112, D01304, doi:10.1029/2005JD006404, 2007.

Feng, Y. and Ramanathan, V.: Investigation of aerosol–cloud interactions using a chemical transport model constrained by satellite observations, Tellus B, 62, 69–86, 2010.

Forster, P., Ramaswamy, V., Artaxo, P., Berntsen, T., Betts, R., Fahey, D. W., Haywood, J., Lean, J., Lowe, D. C., Myhre, G., Nganga, J., Prinn, R., Raga, G., Schulz, M., and Van Dorland, R.: Changes in atmospheric constituents and in radiative forcing, in: Climate Change 2007: The Physical Science Basis, Contribution of Working Group I to the Fourth Assessment Report of the Intergovernmental Panel on Climate Change, edited by: Solomon, S., Qin, D., Manning, M., Chen, Z., Marquis, M., Averyt, K. B., Tignor, M., and Miller, H. L., Cambridge University Press, New York, 130–234, 2007.

Ganguly, D., Rasch, P. J., Wang, H., and Yoon, J.: Climate response of the South Asian monsoon system to anthropogenic aerosols, J. Geophys. Res., 117, D13209, doi:10.1029/2012JD017508, 2012.

Ginoux, P., Chin, M., Tegen, I., Prospero, J. M., Holben, B., Dubovik, O., and Lin, S.-J.: Sources and distributions of dust aerosols simulated with the GOCART model, J. Geophys. Res., 106, 20255–20274, 2001.

Hoffer, A., Gelencsér, A., Guyon, P., Kiss, G., Schmid, O., Frank, G. P., Artaxo, P., and Andreae, M. O.: Optical properties of humic-like substances (HULIS) in biomass-burning aerosols, Atmos. Chem. Phys., 6, 3563–3570, doi:10.5194/acp-6-3563-2006, 2006.

Holben, B. N., Eck, T. F., Slutsker, I., Tanre, D., Buis, J. P., Setzer, A., Vermote, E., Reagan, J. A., Kaufman, Y. J., Nakjima, T., Lavenu, F., Jankowiak, I., and Smirnov, A.: AERONE – a federated instrument network and data archive for aerosol characterization, Remote Sens. Environ., 66, 1–16, 1998.

Huang, J., Zhang, C., and Prospero, J. M.: Large-scale effect of aerosols on precipitation in the West African Monsoon region, Q. J. Roy. Meteorol. Soc., 135, 581–594, doi:10.1002/qj.391, 2009.

Jacobson, M. Z.: Global direct radiative forcing due to multicomponent anthropogenic and natural aerosols, J. Geophys. Res., 106, 1551–1568, 2001.

Jacobson, M. Z.: Short-term effects of controlling fossil-fuel soot, biofuel soot and gases, and methane on climate, Arctic ice, and air pollution health, J. Geophys. Res., 115, D14209, doi:10.1029/2009JD013795, 2010.

ACPD
13, 2795–2833, 2013

Kettle, A. J. and Andreae, M. O.: Flux of dimethylsulfide from the oceans: a comparison of updated data seas and flux models, J. Geophys. Res.-Atmos., 105, 26793–26808, 2000.
Kim, D. and Ramanathan, V.: Solar radiation budget and radiative forcing due to aerosols and clouds, J. Geophys. Res., 113, D02203, doi:10.1029/2007JD008434, 2008.
Kinne, S., Schulz, M., Textor, C., Guibert, S., Balkanski, Y., Bauer, S. E., Berntsen, T., Berglen, T. F., Boucher, O., Chin, M., Collins, W., Dentener, F., Diehl, T., Easter, R., Feichter, J., Fillmore, D., Ghan, S., Ginoux, P., Gong, S., Grini, A., Hendricks, J., Herzog, M., Horowitz, L., Isaksen, I., Iversen, T., Kirkevåg, A., Kloster, S., Koch, D., Kristjansson, J. E., Krol, M., Lauer, A., Lamarque, J. F., Lesins, G., Liu, X., Lohmann, U., Montanaro, V., Myhre, G., Penner, J., Pitari, G., Reddy, S., Seland, O., Stier, P., Takemura, T., and Tie, X.: An AeroCom initial assessment – optical properties in aerosol component modules of global models, Atmos. Chem. Phys., 6, 1815–1834, doi:10.5194/acp-6-1815-2006, 2006.
Kirchstetter, T. W. and Thatcher, T. L.: Contribution of organic carbon to wood smoke particulate matter absorption of solar radiation, Atmos. Chem. Phys., 12, 6067–6072, doi:10.5194/acp-12-6067-2012, 2012.
Kirchstetter, T. W., Novakov T., and Hobbs P. V.: Evidence that the spectral dependence of light absorption by aerosols is affected by organic carbon, J. Geophys. Res., 109, D21208, doi:10.1029/2004JD004999, 2004.
Koch, D., Schulz, M., Kinne, S., McNaughton, C., Spackman, J. R., Balkanski, Y., Bauer, S., Berntsen, T., Bond, T. C., Boucher, O., Chin, M., Clarke, A., De Luca, N., Dentener, F., Diehl, T., Dubovik, O., Easter, R., Fahey, D. W., Feichter, J., Fillmore, D., Freitag, S., Ghan, S., Ginoux, P., Gong, S., Horowitz, L., Iversen, T., Kirkevåg, A., Klimont, Z., Kondo, Y., Krol, M., Liu, X., Miller, R., Montanaro, V., Moteki, N., Myhre, G., Penner, J. E., Perlwitz, J., Pitari, G., Reddy, S., Sahu, L., Sakamoto, H., Schuster, G., Schwarz, J. P., Seland, Ø., Stier, P., Takegawa, N., Takemura, T., Textor, C., van Aardenne, J. A., and Zhao, Y.: Evaluation of black carbon estimations in global aerosol models, Atmos. Chem. Phys., 9, 9001–9026, doi:10.5194/acp-9-9001-2009, 2009.
Limbeck, A., Kulmala, M., and Puxbaum, H.: Secondary organic aerosol formation in the atmosphere via heterogeneous reaction of gaseous isoprene on acidic particles, Geophys. Res. Lett., 30, 1996, doi:10.1029/2003GL017738, 2003.
Lin, S.-J. and Rood, R. B.: Multidimensional flux-form semi-Lagrangian transport schemes, Mon. Weather Rev., 124, 2046–2070, 1996.

ACPD
13, 2795–2833, 2013

Liu, H., Jacob, D. J., Bey, I., and Yantosca, R. M.: Constraints from ^{210}Pb and ^{7}Be on wet deposition and transport in a global threedimensional chemical tracer model driven by assimilated meteorological fields, J. Geophys. Res., 106, 12109–12128, 2001.

Liu, X. and Penner, J. E.: Effect of Mt. Pinatubo H_2SO_4/H_2O aerosol on ice nucleation in the upper troposphere using a global chemistry and transport model (IMPACT), J. Geophys. Res., 107, D124141, doi:10.1029/2001JD000455, 2002.

Liu, X., Penner, J. E., and Herzog, M.: Global simulation of aerosol dynamics: model description, evaluation, and interactions between sulfate and nonsulfate aerosols, J. Geophys. Res., 110, D18206, doi:10.1029/2004JD005674, 2005.

Liu, X., Penner, J. E., Das, B., Bergmann, D., Rodriguez, J. M., Strahan, S., Wang, M., and Feng, Y.: Uncertainties in global aerosol simulations: assessment using three meteorological datasets, J. Geophys. Res., 112, D11212, doi:10.1029/2006JD008216, 2007.

Menon, S., Koch, D., Beig, G., Sahu, S., Fasullo, J., and Orlikowski, D.: Black carbon aerosols and the third polar ice cap, Atmos. Chem. Phys., 10, 4559–4571, doi:10.5194/acp-10-4559-2010, 2010.

Ming, Y., Ramaswamy, V., and Persad, G.: Two opposing effects of absorbing aerosols on global-mean precipitation, Geophys. Res. Lett., 37, L13701, doi:10.1029/2010GL042895, 2010.

Monahan, E. C., Spiel, D. E., and Davidson, K. L.: A Model of Marine Aerosol Generation via Whitecaps and Wave Disruption, D. Reidel, Norwell, MA, 1986.

Mukai, H. and Ambe, Y.: Characterization of a humic acid-like brown substance in airborne particulatematter and tentative identification of its origin, Atmos. Environ., 20, 813–819, 1986.

Olivier, J. G. J. and Berdowski, J. J. M.: Global emissions sources and sinks, in: The Climate System, edited by: Berdowski, J., Guicherit, R., and Heij, B. J., A. A. Balkema Publishers/Swets & Zeitlinger Publishers, Lisse, The Netherlands, 33–78, 2001.

Olivier, J. G. J., Berdowski, J. J. M., Peters, J., Bakker, J., Visschedijk A., and Bloos, J.: Applications of EDGAR. Including a description of EDGAR 3.0: reference database with trend data for 1970–1995, RIVM report no. 773301 001/NOP report no. 410200 051, RIVM, Bilthoven, 2001.

Park, R. J., Kim, M. J., Jeong, J. I., Youn, D., and Kim, S.: A contribution of brown carbon aerosol to the aerosol light absorption and its radiative forcing in East Asia, Atmos. Environ., 44, 1414–1421, 2010.

ACPD
13, 2795–2833, 2013

Penner, J. E., Chuang, C., and Grant, K.: Climate forcing by carbonaceous and sulfate aerosols, Clim. Dynam., 14, 839–851, 1998.
Podgorny, I. A. and Ramanathan, V.: A modeling study of the direct effect of aerosols over the tropical Indian Ocean, J. Geophys. Res., 106, 24097–24105, 2001.
Radke, L. F., Hegg, D. A., Lyons, J. H., Brock, C. A., Hobbs, P. V., Weiss, R. E., and Rasmussen, R. A.: Airborne Measurements on Smoke from Biomass Burning, A. Deepak, Hampton, VA, 1988.
Ramanathan, V. and Carmichael, G.: Global and regional climate changes due to black carbon, Nat. Geosci., 1, 221–227, 2008.
Rotman, D. A., Atherton, C. S., Bergmann, D. J., Cameron-Smith, P. J., Chuang, C. C., Connell, P. S., Dignon, J. E., Franz, A., Grant, K. E., Kinnison, D. E., Molenkamp, C. R., Proctor, D. D., and Tannahill, J. R.: IMPACT, the LLNL 3-D global atmospheric chemical transport model for the combined troposphere and stratosphere: model description and analysis of ozone and other trace gases, J. Geophys. Res., 109, D04303, doi:10.1029/2002JD003155, 2004.
Russell, P. B., Bergstrom, R. W., Shinozuka, Y., Clarke, A. D., DeCarlo, P. F., Jimenez, J. L., Livingston, J. M., Redemann, J., Dubovik, O., and Strawa, A.: Absorption Angstrom Exponent in AERONET and related data as an indicator of aerosol composition, Atmos. Chem. Phys., 10, 1155–1169, doi:10.5194/acp-10-1155-2010, 2010.
Sakaeda, N., Wood, R., and Rasch, P. J.: Direct and semidirect aerosol effects of southern African biomass burning aerosol, J. Geophys. Res.-Atmos., 116, D12205, doi:10.1029/2010JD015540, 2011.
Sato, M., Hansen, J., Koch, D., Lacis, A., Ruedy, R., Dubovik, O., Holben, B., Chin, M., and Novakov, T.: Global atmospheric black carbon inferred from AERONET, P. Natl. Acad. Sci. USA, 100, 6319–6324, doi:10.1073/pnas.0731897100, 2003.
Schulz, M., Textor, C., Kinne, S., Balkanski, Y., Bauer, S., Berntsen, T., Berglen, T., Boucher, O., Dentener, F., Guibert, S., Isaksen, I. S. A., Iversen, T., Koch, D., Kirkevåg, A., Liu, X., Montanaro, V., Myhre, G., Penner, J. E., Pitari, G., Reddy, S., Seland, Ø., Stier, P., and Takemura, T.: Radiative forcing by aerosols as derived from the AeroCom present-day and pre-industrial simulations, Atmos. Chem. Phys., 6, 5225–5246, doi:10.5194/acp-6-5225-2006, 2006.
Shindell, D. and Faluvegi, G.: Climate response to regional radiative forcing during the twentieth century, Nat. Geosci., 2, 294–300, doi:10.1038/NGEO473, 2009.
Shindell,D., Kuylenstierna, J. C. I., Vignati, E., van Dingenen, R., Amann, M., Klimont, Z., Anenberg, S. C., Muller, N., Janssens-Maenhout, G., Raes, F., Schwartz, J. Faluvegi, G., Pozzoli,

ACPD
13, 2795–2833, 2013

L., Kupiainen, K., Höglund-Isaksson, L., Emberson, L., Streets, D., Ramanathan, V., Hicks, K., Kim Oanh, N. T., Milly, G., Williams, M., Demkine, V., and Fowler, D.: Simultaneously mitigating near-term climate change and improving human health and food security, Science, 335, 183–189, 2012.

Torres, O., Tanskanen, A., Veihelmann, B., Ahn, C., Braak, R., Bhartia, P. K., Veefkind, P., and Levelt, P.: Aerosols and surface UV products from Ozone Monitoring Instrument observations: an overview, J. Geophys. Res., 112, D24S47, doi:10.1029/2007JD008809, 2007.

Uppala, S. M., Kållberg, P. W., Simmons, A. J., Andrae, U., Bechtold, V. D. C., Fiorino, M., Gibson, J. K., Haseler, J., Hernandez, A., Kelly, G. A., Li, X., Onogi, K., Saarinen, S., Sokka, N., Allan, R. P., Andersson, E., Arpe, K., Balmaseda, M. A., Beljaars, A. C. M., Berg, L. V. D., Bidlot, J., Bormann, N., Caires, S., Chevallier, F., Dethof, A., Dragosavac, M., Fisher, M., Fuentes, M., Hagemann, S., Hólm, E., Hoskins, B. J., Isaksen, L., Janssen, P. A. E. M., Jenne, R., Mcnally, A. P., Mahfouf, J.-F., Morcrette, J.-J., Rayner, N. A., Saunders, R. W., Simon, P., Sterl, A., Trenberth, K. E., Untch, A., Vasiljevic, D., Viterbo, P., and Woollen, J.: The ERA-40 re-analysis, Q. J. Roy. Meteorol. Soc., 131, 2961–3012, 2005.

Vogelmann, A. M., Ramanathan, V., and Podgorny, I. A.: Scale dependence of solar heating rates in convective cloud systems with implications to General Circulation Models, J. Climate, 14, 1738–1752, 2001.

Zhang, L., Gong, S. L., Padro, J., and Barrie, L.: A size-segregated particle dry deposition scheme for an atmospheric aerosol module, Atmos. Environ., 35, 549–560, 2001.

ACPD

13, 2795–2833, 2013

Table 1. Annual emissions and burdens of anthropogenic aerosols and their lifetimes, simulated for year 2000[a].

	Sulfate	Black Carbon	Organic Matter	Brown Carbon
Total Emissions:	96.14 Tg S FF: 56.2 Volcanoes: 14.6 DMS: 25.3	7.96 Tg C FF: 3.15 BF: 1.77 BB: 3.04	69.5 Tg FF: 4.5 BF: 11.2 BB: 34.7 Natural: 19.1	– –
Burden: mg m^{-2} (AeroCom estimates)[b]	4.7 (mean: 3.9 min: 1.8 max: 5.3)	0.19 (mean: 0.39 min: 0.09 max: 1.0)	1.5 (mean: 3.3 min: 0.9 max: 5.0)	0.65
Lifetime: days	3.04	4.45	4.02	–

[a] FF: fossil fuel combustion; BF: biofuel combustion; BB: biomass burning.
[b] Kinne et al. (2006).

ACPD
13, 2795–2833, 2013

Table 2. The imaginary refractive index, absorption cross section, and absorption Angstrom exponent (AAE) calculated for brown carbon (BrC) at various wavelengths.

	Imaginary refractive index at indicated wavelength				Absorption cross section at indicated wavelength ($m^2\,g^{-1}$)				AAE
Wavelength (nm)	350	450	550	650	350	450	550	650	400–700
Moderately absorbing BrC[a]	0.075	0.02	0.003	0.0003	2.25	0.63	0.08	0.006	11.1
Strongly absorbing BrC[b]	0.168	0.063	0.03	0.005	3.40	1.60	0.70	0.10	6.6

[a] Absorption cross section based on Chen and Bond (2010).
[b] Based on Kirchstetter et al. (2004).

ACPD
13, 2795–2833, 2013

Table 3. Global and annual mean absorbing aerosol optical depth (AAOD) and absorption Angstrom exponent (AAE) at various wavelengths. The percentage increase in AAOD with the inclusion of BrC is indicated by numbers in parentheses.

	AAOD at indicated wavelength				AAE
Wavelength	350 nm	450 nm	550 nm	650 nm	440–870 nm
Without BrC	0.0045	0.0039	0.0034	0.0029	0.9
Moderately absorbing BrC	0.0062 (+38 %)	0.0042 (+8 %)	0.0035 (+3 %)	0.003 (+3 %)	1.0
Strongly absorbing BrC	0.007 (+56 %)	0.0049 (+26 %)	0.004 (+18 %)	0.003 (+3 %)	1.2

ACPD
13, 2795–2833, 2013

Table 4. Global and annual mean aerosol (fossil fuel, biofuel, and biomass burning) direct forcing for year 2000. Numbers in parentheses indicate the percent of the total aerosol forcing.

$W m^{-2}$	All aerosols (this work)	All aerosols (AeroCom)[a]	RC2008[b] (Observation-constrained)	BrC	BC	Other aerosols
TOA	−0.17	−0.22	−0.4	0.04–0.11	0.45	−0.66
Atmosphere	1.47	0.82	3.0	0.1–0.25 (7–19 %)	1.07 (72 %)	0.13 (9 %)
Surface	−1.64	−1.02	−3.4	−0.06 to −0.14 (4–11 %)	−0.62 (41 %)	−0.79 (48 %)

[a] Schulz et al. (2006).
[b] RC2008: Ramanathan and Carmichael (2008).

ACPD
13, 2795–2833, 2013

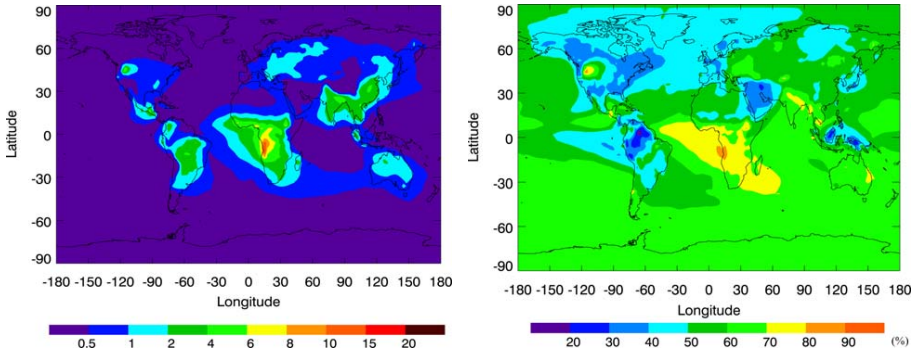

Fig. 1. The estimated **(a)** annual mean atmospheric burden ($mg\,m^{-2}$) of BrC and **(b)** fraction (in %) of BrC in total OC.

ACPD
13, 2795–2833, 2013

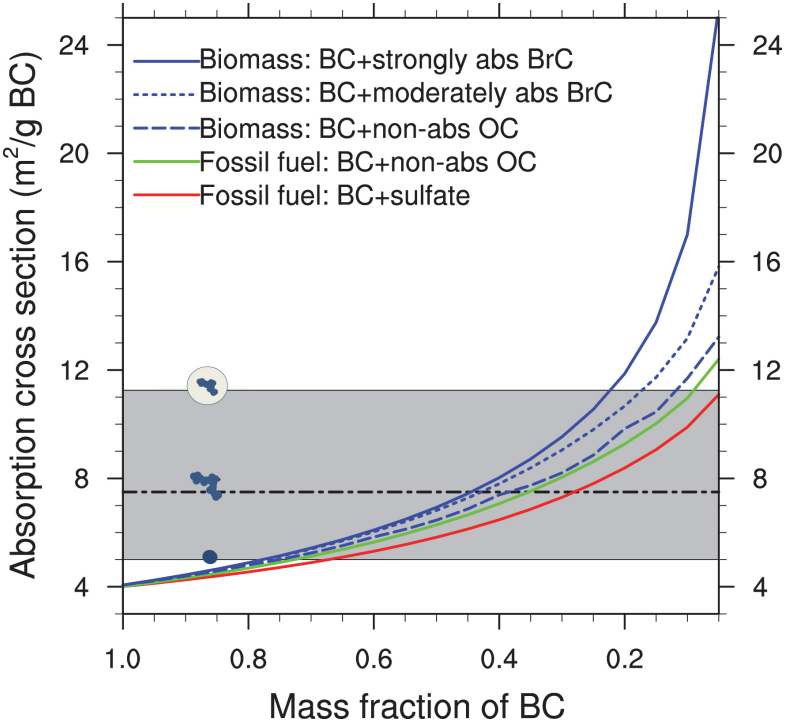

Fig. 2. The enhancement in absorption cross section ($m^2\,g^{-1}$ BC) at 550 nm, calculated for coated BC particles in dry conditions. The composition of the coating material is assumed to be sulfate (red) or non-absorbing OC (green) for fossil fuel aerosol. For biofuel and biomass burning aerosols the coating is non-absorbing OC (blue dashed), or moderately absorbing BrC (blue dotted; Chen and Bond, 2010), or strongly absorbing BrC (blue solid; Kirchstetter et al., 2004). Also shown in gray shading are values for freshly emitted BC particles ($5\,m^2\,g^{-1}$), aggregates ($7.5\,m^2\,g^{-1}$), and aged BC with coatings ($11.25\,m^2\,g^{-1}$) recommended in Bond and Bergstrom (2006) and Bond et al. (2006).

ACPD
13, 2795–2833, 2013

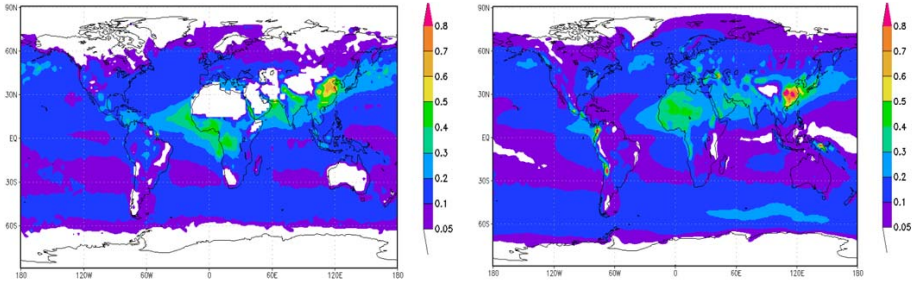

(a) (b)

Fig. 3. Annual mean aerosol optical depth from **(a)** MODIS/Terra satellite observations (2001) and **(b)** model simulations. The white color in **(a)** indicates the areas over which satellite retrievals are not available.

ACPD
13, 2795–2833, 2013

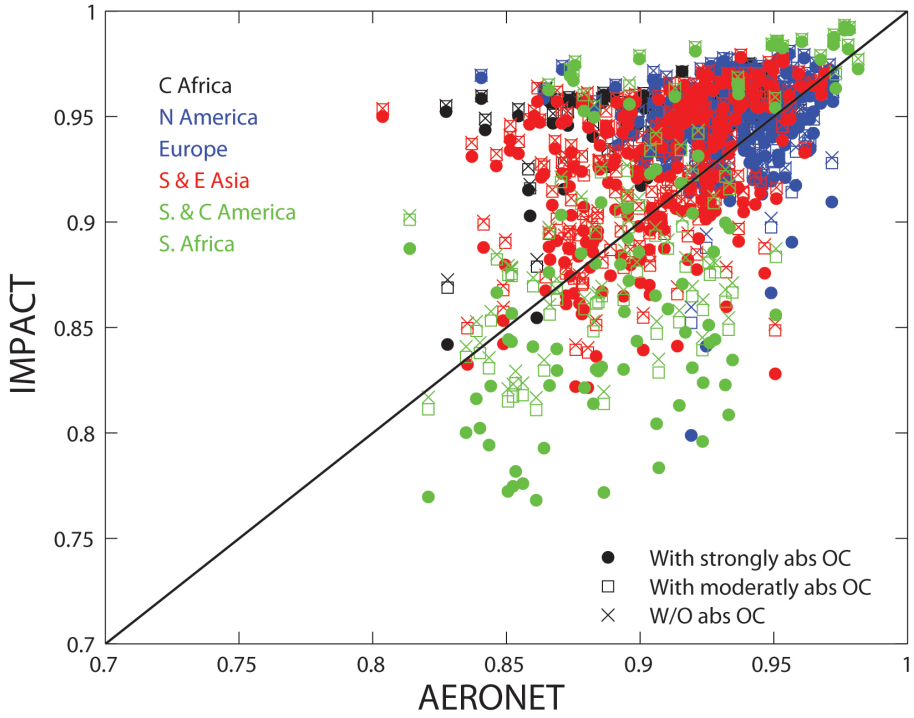

Fig. 4. Comparison of monthly mean SSA at 550 nm from AERONET (1992–2012) and model simulations. The solid line indicates the 1 : 1 ratio. Data points in central Africa (C. Africa), Europe and North America, South Asia and East Asia (S and E Asia) and regions dominated by biomass burning (South and Central America (S and C America) and southern Africa (S. Africa)) are colored in black, blue, red, and green, respectively. Symbols denote the model sensitivity studies with different BrC properties.

ACPD
13, 2795–2833, 2013

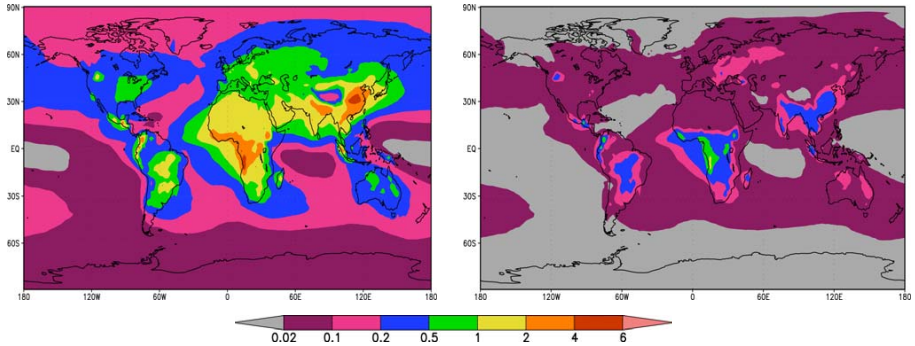

Fig. 5. (Left) Annual mean absorption aerosol optical depth (AAOD ×100) calculated with strongly absorbing BrC included (Kirchstetter et al., 2004). (Right) increases in AAOD (×100) due to BrC.

ACPD
13, 2795–2833, 2013

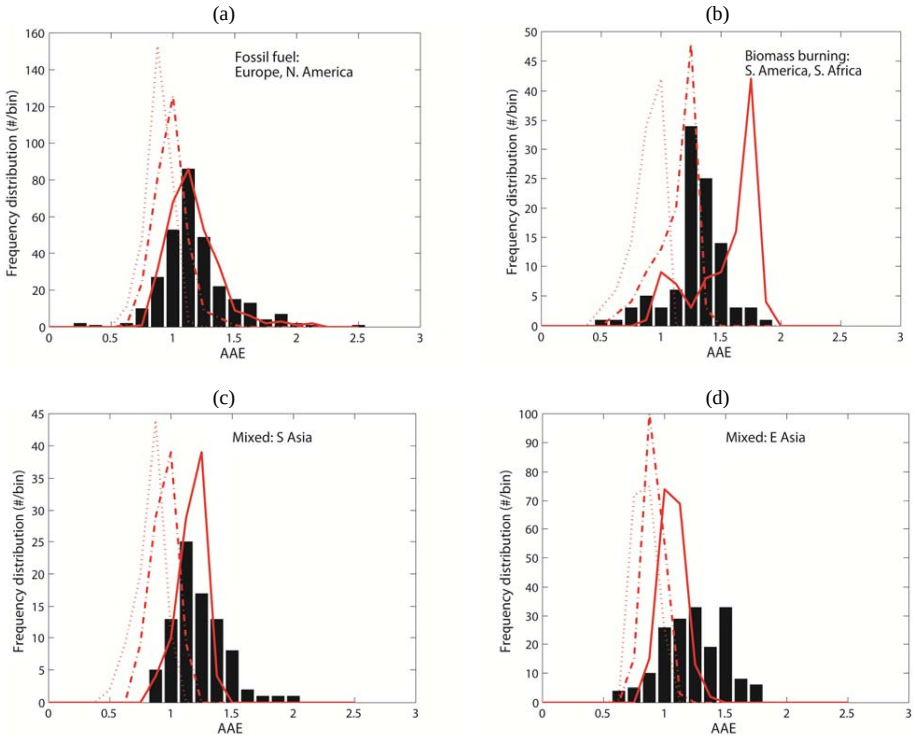

Fig. 6. Frequency distribution of the aerosol absorption angstrom exponent (AAE) at 440–870 nm, derived from the AERONET data (bar) and model simulations (in red). Dotted line, no BrC; dash-dot line, moderately absorbing BrC; solid line, strongly absorbing BrC at 775 total AERONET sites. Distributions are over **(a)** fossil fuel-dominated Europe and North America, **(b)** open biomass burning-dominated South America and southern Africa, **(c)** mixed source region in South Asia, and **(d)** mixed source region in East Asia.

ACPD
13, 2795–2833, 2013

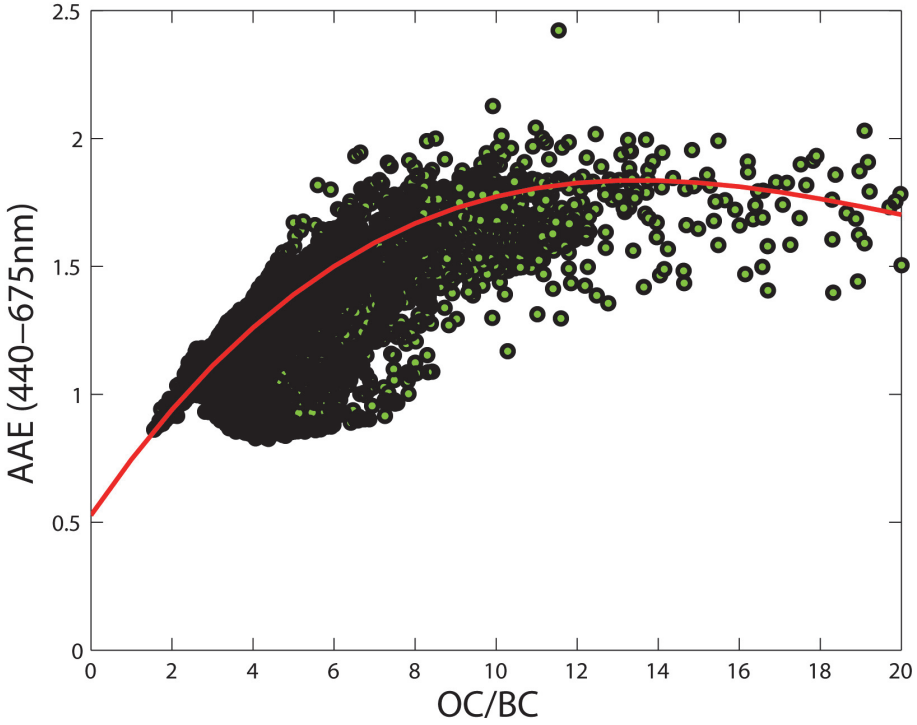

Fig. 7. In the global simulations with strongly absorbing BrC, AAE (440–675 nm) as a function of the ratio of OC burden to BC. Solid red line is the best-fit curve.

ACPD
13, 2795–2833, 2013

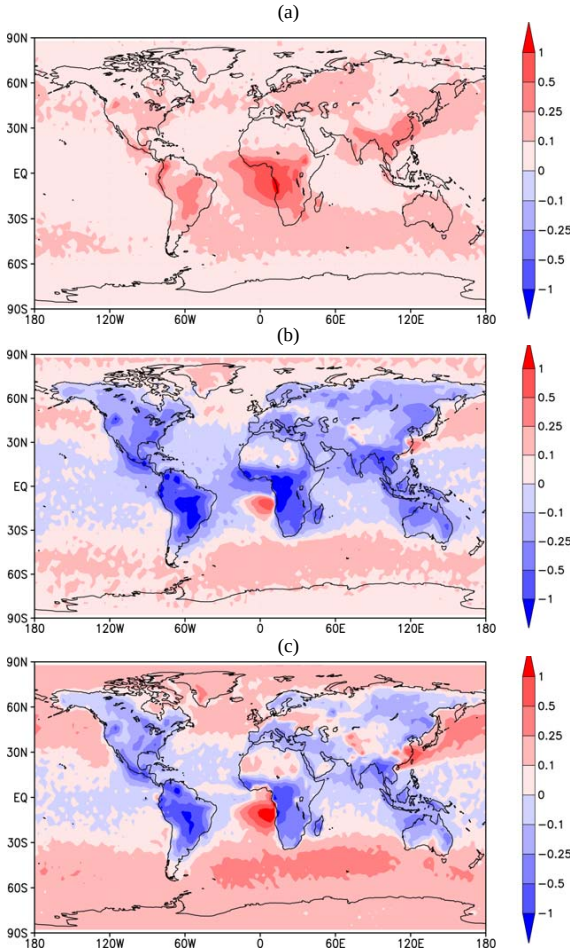

Fig. 8. The estimated annual mean all-sky direct radiative forcing ($W m^{-2}$) by **(a)** BrC, **(b)** organic aerosols without BrC, and **(c)** organic aerosols with BrC, at the top of the atmosphere.

ACPD
13, 2795–2833, 2013

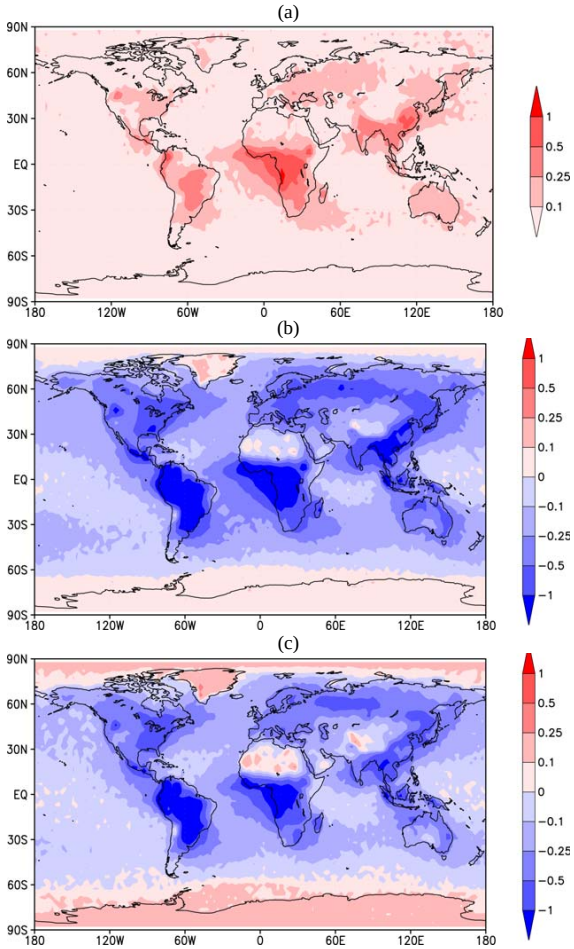

Fig. 9. As for Fig. 8, but for clear-sky forcing.

ACPD
13, 2795–2833, 2013

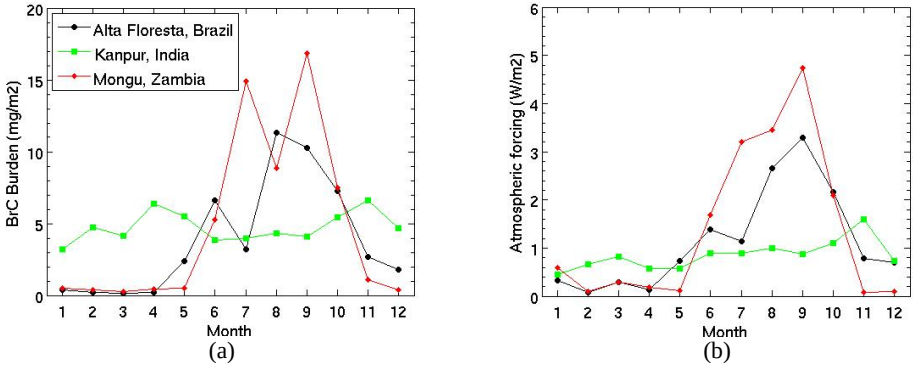

Fig. 10. Seasonal variations in the model predictions of **(a)** BrC burden ($mg\,m^{-2}$) and **(b)** atmospheric absorption ($W\,m^{-2}$) at Alta Floresta, Brazil (56.1° W, 9.87° S), Kanpur, India (80.23° E, 26.51° N), and Mongu, Zambia (23.15° E, 15.25° S).

ACPD
13, 2795–2833, 2013